ISTITUTO NAZIONALE DI FISICA NUCLEARE

Sezione di Genova

INFN/TC-02/05
4 Aprile 2002

AN ULTRA-LIGHT COMPOSITE STRUCTURE TO SUPPORT ELECTRONIC DEVICES IN A SYNCHROTRONE PARTICLE DETECTOR

Stefano Cuneo[1], Roberto Cereseto[2], Flavio Gastaldo[2], Flavio Mora[3], Marco Olcese[2], Claudio Pizzorno[2], Rosanna Puppo[2],

[1)]INFN-Sezione di Genova, Via Dodecaneso 33 - 16146 Genova, Italy
fax 00 39 010 313358 - Email stefano.cuneo@ge.infn.it
[2)] INFN-Sezione di Genova, Via Dodecaneso 33 - 16146 Genova, Italy
[3)]Plyform S.r.L. - Via Diaz 24 - Bienate di Magnago (MI) - Italy

Abstract

This paper describes the extensive program of activity carried out to design, qualify and optimize the composite support structures (staves) for the sensitive elements of the ATLAS Pixel Detector to be installed in the new Large Hadron Collider at CERN.

Design consideration, structural and thermal simulations and test covered all critical aspect of the components, finding a good agreement, so that the requirements in operation are expected to be met; the results are reported in detail.

PACS.: insert the exact ref. number

Published by ***SIS–Pubblicazioni***
Laboratori Nazionali di Frascati

1 INTRODUCTION

The needs of experimental physics of particles leads the scientific community to ask for new detectors having increasingly high resolution close to the point where the reaction happens. At the same time, as other detectors often surround the inner one and need to receive as much as possible the same particles with the same energy, the mechanical supports that have to support the detecting electronics must be extremely light, to minimise the mass that could shield the particles to the outer detectors.

Nevertheless, these structures must fulfil other tasks, as drain the heat generated by the electronics, precisely locate the detectors in the space and remain stable under operating conditions, that means static and dynamic loads joined with temperature difference.
While they wouldn't be in an usual structure, the loads become extremely severe where you have to reduce at a minimum the dimensions. That's the reason why we investigated the application of composite materials, that can join stiffness and lightness. The final design we could produce will be used to manufacture parts of the Atlas Pixel Inner Detector [1), 2)] in the new LHC synchrotrone facility under construction at CERN, Geneva.

2 CONSTRAINTS AND REQUIREMENTS

The structure we're discussing of was expected to carry 13 electronic devices (see fig. 1) glued on it, to form a sort of continuous strip of their detecting active areas (fig. 2). Any of these devices had a weight of around 3 grams and, in operating conditions, generates a heat load of around 11 W.

The temperature on the device surface during operation couldn't exceed –6°C, while the environment was kept a –10°C. Then provision had to be made to foresee a leak tight structure that housed a closed channel where the needed coolant could flow. A separate study [3)] showed that the best choice was an evaporative cooling system based on C3F8, that meant that the expected pressure inside the above mentioned channel could range from 2 to 4 bar abs during normal operation, while it could reach 10 bar abs in system fault condition. The required mass flow rate and the allowable pressure drop fixed the hydraulic diameter of the channel at 4.7 mm.

As the structure had to be submitted to the action of high energy particles, a basic requirements was that all the materials used in the construction were "radiation hard", that means that they had to prove that their mechanical properties wouldn't significantly decay once they've been exposed to the expected amount of radiation energy. Required lifetime is 10 years of operation.

The structure wasn't a stand alone one, but it was foresee to be surrounded by many of the same type (see fig. 3), to form a "barrel" that could capture as much as possible the particles produced in the centre of interaction from a defined energy level up. That constraint forced us to design a layout where the packing factor was very low, that means that clearances an gaps were minimised. Furthermore, the experiment couldn't afford to have a large spread around the design minimum value of captured particles energy. All that lead us

to specify as acceptance criterion for the structure accuracy, based on the manufacturing and assembling accuracy, a deviation in linearity of ±0.25 mm.

As the operating temperature was 30°C below the assembling temperature, and different materials (at least the electronic devices, their glue layer and the mechanical support) had to be joined together, the bi-laminar effect due to the unavoidable CTE (coefficient of temperature expansion) mismatch had to be minimised, to ensure that the geometry in operation couldn't deviate too much from the ideal one. As the accuracy in locating particles in space was one of the main goals of the experiment, we were forced to set as acceptance criterion for the structure thermal stability a deviation in linearity of ±0.020 mm.

For the same reasons, the choice of the materials had to consider that a minimum swelling due to moisture absorption of the structure could be allowed.

Dynamic loads were not specified, nor was easy to foresee them. Then, to be sure to avoid any resonance, we set as dynamic stability acceptance criterion that the first modal frequency of the structure should stay above 100 Hz.

Last but not least, the mass of the structure had to be minimised, and preference given to those material having better particle transparency, not to shield too much the particle to the outer detectors. In table 1 you can find a summary of main constraints and requirements.

3 CHOICE OF THE MATERIALS

Previous experience made in similar application, as well as some preliminary, very obvious, considerations, lead us to circumscribe the choice of the material to those listed in the table below; where aluminium is shown just for comparison. Table 2 is a summary of the material characteristics that, as well as their proved radiation hardness, drove the choice. Note that the radiation length X_0, that should be as large as possible for better particle transparency, has been one of the most important acceptance criterion.

Getting into detail of the various materials:

- C-C: lay up of 22 layers of carbon fibres fabric in phenolic resin matrix, twice densified and then graphitised at high temperature. This material, available in plates, can be satisfactory machined to the required shape, provided that high speed (up to 40000 rpm) of the tool can be set; the C-C features good transverse thermal conductivity, very high radiation length, excellent stiffness and stability, low CTE. The porosity is the only drawback of such a material, but has been overcome by a custom-developed impregnation process [6)], providing the required leak-tightness even at very small thickness (0.4 mm minimum).
- Carbon fibres (pre-preg): the part of the structure where the coolant has to flow is made of three layers of unidirectional UHM carbon fibre reinforced cyanate ester resin pre-preg. The adopted lay-up (0-90-0), 0.3 mm thick, has been optimised through an extensive design and test program. The choice of the pre-preg material and of the lay-up has been done in order to achieve a longitudinal CTE of the part

as close as possible to the CTE of the impregnated C-C, to minimise the distortions due to the cool down. The achieved longitudinal CTE mismatch, less than 1 ppm, allows the structure to fully meet the stability requirements. After the lay-up. The fibres are formed to the required shape by means of a graphite mould, whose optimisation, as well as the fibres manufacturing process set-up, have been carried out during an extensive development program.

- Ciba glue Araldite 420 A/B: the carbon fibre profile is sealed on the C-C part using this glue, that features a very high peeling strength. The strength and reliability of the adhesive joint, one of the most critical point of the design, have been deeply investigated and qualified through a very extensive destructive and long term test program, on both test specimens an part of real-scale prototypes, that is discussed in a another paper.

4 OVERVIEW OF THE GEOMETRY

The structure could be roughly defined as monolithic full carbon based; it consists basically of two parts: a Thermal Management Tile (TMT) and an omega piece (see figure 4) with an integrated cooling channel. The TMT is machined out of a Carbon-Carbon (C-C) bar shaped in a series of 12 shingled steps symmetrically displaced (6 each side) around a central flat step. Every step will locate an electronic sensor (module); the shingled geometry allows for overlap between the 13 modules hosted on the stave, to achieve the required particle coverage. At earlier stages of the project the geometry of the TMT consisted of a two-level parallel stepping sequence; this geometry was proposed due to easy machining and survey, but has been abandoned for the shingled geometry, that allows for a full compatibility of the two module types currently under study. The adopted design changes resulted in improvements in rigidity and stability, because of the larger bending stiffness of the transverse section. In order to reduce the mass, slots are machined on the side of the stave; then, the thinner parts of the stave are 0.4 mm thick. For better handling during the shop operations, the TMT is made in two halves of around 400 mm length, that are glued together just before the omega profile is glued on their backside. The final piece looks like a bar of around 800 mm length.

That structure, that we'll call "stave", is supported at three points, by means of one rigidly connected support at the central point and two removable supports at the two ends.

Two staves are mounted on common supports to form a bi-stave assembly; at this stage the cooling pipe connections are put in place and the bi-stave assembly is then ready for the installation into the half shell structure (see figure 5), to form the so-called "layers".

The staves of layer 1 and 2 are foreseen to be supported by a shell barrel composite structure made of a 0.4 mm thick carbon fiber shell glued onto three carbon-carbon supporting rings, where the bi-staves will be screwed on (see fig. 6). Every layer will have its own shell that is made of two halves, to be joined together by means of screws and dowel pins. This solution should allow for easier assembling and survey of the staves.

5 STRUCTURAL SIMULATION AND MEASUREMENTS

Modeling techniques and details

The stave FEA model has been set up to run under ANSYS Multiphysics version 5.5.2 [5]. The global reference system has been oriented with its X axis parallel to the major dimension (length) of the structure, while Y and Z axis were parallel to the thickness and the width respectively.

A mapped mesh (see fig. 7) was required, very fine because of the small thickness of the different materials (0.1 mm for the glue layers, 0.3 mm for the omega profile, 0.4 mm for the c-c tile). Where possible, a plane meshing have been done and then extruded into a volume. The origin have been set in a position convenient for extrusion along Z of a meshed section. Nevertheless, it has been impossible to avoid at all some elements to collapse beyond the suggested maximum aspect ratio limit, because of the very small angles (1.1°) of the geometry. We didn't consider the relevant warnings the program gave as, in principle, an aspect ratio larger than the suggested value should affect mainly the accuracy of the stress solution, and not too much the displacements, that were the main task of our investigation. Furthermore, only a small percentage of the total amount of elements was out of the suggested aspect ratio range. The measurements (see below) confirmed that, despite of the warnings, the results of the simulation were consistent.

The geometry has been modelled with all its details (fig. 8), except the tool rounding radius and the incline of the Y-Z facets, too small to be significant.

Brick elements have been used to model the parts made of orthotropic materials, while layered brick elements have been used to model the carbon fibre. Special care has been devoted to re-direct the coordinate system of the layered elements in order to be consistent with the actual lay-up of the pre-preg fibres. Due to the large number of elements, an iterative software routine has been set up to do this task.

Central symmetry boundary condition have been set, to reduce the number of elements and speed up the calculations. This trick allowed to limit the total number of nodes to around 56000, with 40000 elements. Except the ends, the structure looks like a series of 6 of an "elementary" volume, that then have been modelled, meshed and copied 6 times in the proper position. Of course, all the pictures attached will show only one half of the structure.

Finally, the constraints have been modelled setting to zero the relevant displacements (UX=UY=UZ=0 in case of restrained joint, UY=UZ=0 in case of hinge on a sliding shoe) of all the relevant nodes. We considered two constraints schemes (see fig. 9): scheme "A", close to the situation we reproduced on the support we used to measure the prototypes, and scheme "B", more restrained. The elements we used didn't feature any rotation as nodal degree of freedom.

Material properties

Five different materials are used in the structure of the stave. Their properties are discussed below, and the main numeric values we used are summarised in table 3.

- Carbon fibres:.the CTE value along the x direction was modified so that the simulation of the stand-alone omega profile could match the measured CTE of the global structure along the length (X direction), whose value is –0.39e-6 [4]. The mechanical properties, and in particular the shear modulus, were instead derived with classical Schneider's lamination theory [7].
- CIBA glue Araldite 420 A/B: we assumed isotropic properties for it.
- Impregnated carbon-carbon: two different carbon-carbons have been considered, from different supplier (BF Goodrich and SGL Carbon). Though BF Goodrich features a Young's modulus along the X direction close to twice SGL's, in all the simulations we made the difference looked to be negligible, probably because it gives a minor contribution to the stiffness of the global structure. We assumed that the resin introduced in the material to fill its porosity and seal it (around 10% in weight) didn't affect the elastic properties of the materials, and then we used the Supplier's Young's modulus. On the contrary, even such small amount of resin has heavy influence on the CTE: the measurements committed to a specialized firm confirmed it [4], and allowed us to introduce in the calculations the right value.
- CGL 7018 glue: is the glue that bonds the electronic components to the carbon-carbon tile. It has been selected to ensure a good thermal contact but the poorest mechanical coupling of the electronics with the stave, because of the large CTE mismatch, that could induce deformations of the structure.
- Silicone: we simplified the structure of the electronic modules, considering them as a piece of homogeneous silicone. Its density have been changed, to simulate the mass of the actual electronic devices.

Structural simulations

The model has been calculated first at all with a load at a time, to separate the effects and identify the individual contributions, then with all the loads together, to simulate the actual operating conditions. Only displacements along Y have been considered, that is the most concerning aspect of the behaviour of the structure. We simulated the structure restrained as per scheme "A" (fig. 9), that means in the less restrained situation. Therefore, as the actual constraint scheme should try to approach as much as possible the "B" scheme, the results we found should include a safety margin. Hereafter you'll find a discussion of all the load conditions.

- Gravity: we simulated the gravity acceleration as acting along the negative Y axis. Due to the bending stiffness of the structure on Z, quite smaller than on Y, this is largely the worst case. We didn't consider the mass of the coolant inside, as the actual structure will be connected to an evaporative system, and only a small mass contribution is expected to come from the partly evaporated liquid that should flow

inside. Then the total mass of the stave was 0.107 Kg. Generally speaking, a 0.022 mm maximum deflection (fig. 10) is quite small and confirms the good stiffness of the structure. The structure shows a twist of the section: further simulations on a simplified model confirmed such a behaviour, probably due to the marked asymmetry of the cross section.

- Cool down: we simulated the structure when cooled down from 20°C (assembling temperature) to –10°C (operating ambient temperature). The structure assumed an "S" shape (see fig. 11) with positive displacements, accordingly with the expected bi-laminar effect due to the CTE mismatch (the c-c tile features a larger CTE along X direction than the omega profile, considering the absolute values) and the type of constraint (hinge on a sliding shoe) at the end.
- Combined load: we simulated the contemporary action of the loads studied above. The results showed that, when acting in the opposite direction of the thermal displacements, the gravity almost cancels the thermal effects (fig. 12), while it doubles them when acting in the same direction (fig. 13). Both situation can happen in the actual supporting structure, but anyway the structure is stiff enough to meet the requirements.

Modal analysis

A modal analysis have been performed to check whether such a structure could comply with the requirement of a first modal frequency above 100 Hz. The structure has been considered with its own mass (0.107 Kg, including the electronic devices glued on) plus the coolant that could fill the channel (0.040 Kg). The simulations, whose results are summarised in table 4, have been done in two constraint schemes. As expected from the theory, the more restrained structure gave the higher frequencies.

The actual constraint will probably have a behaviour in between the restrained joint and the hinge on a sliding shoe; therefore, the actual first modal frequency should be between 105 and 148 Hz.

Measurements

Several real scale prototypes of stave have been assembled, and the model has been validated by means of measurements of bowing under a known load.

First at all, a static measurement has been done on a prototype, constraining it as simple resting beam, applying a known load in the midst of its span and measuring the relevant deflection. Then the structure has been simulated in the same constraints scheme and load condition, finding a deflection with around 3% of error in excess, compared to the measured one, that had been judged satisfactory for the task of our investigation.

Measurements on prototypes, constrained as per scheme "A", have been made also before and after cooling down from room temperature to –10°C, to check the vertical displacements due to the temperature fall (see fig. 14). The stave have been placed in a cold

box resting on the operating bench of a CMM machine with an individual point accuracy of 0.003 mm. All the stave supports were mounted on quartz columns to have an excellent stability during the cool down and they were provided with load cells to monitor the reacting forces. Though always meeting the requirements, the measures didn't completely fit with the calculations. This can probably be explained with the different amount of resin in the impregnated carbon-carbon (every piece of c-c has its own history, as the impregnation process is not made on an industrial basis, and the c-c tile whose CTE has been measured didn't become a part of a measured stave), that gave it a CTE slightly different from the value set up in the calculations, while the CTE of the omega profiles, all made of the same batch of material, was constant. Therefore the bi-laminar effect produced a bowing sometimes larger or smaller than expected. Nevertheless, the calculated tendency agreed with the actual one, and the model proved to be a good approximation of the actual structure.

6 THERMAL SIMULATIONS AND MEASUREMENTS

Simulations

Finite element thermal analyses were carried out to simulate the heat transmission through the C-C tile and the module glue layer when the coolant is flowing underneath it and the power on the module is on. We modelled only the steps and not the complete structure, assuming that the poor thickness of the c-c tile (0.4 mm) between neighbouring steps wouldn't allow the heat to longitudinally flow through the stave, then insulating each step from the neighbouring ones. We assumed a constant wall temperature on the coolant side, that is consistent with the option of evaporative cooling system, and we estimated the highest temperatures on the module surface ("hot spots", see fig. 15). Different C-C, with different values of transverse thermal conductivity (ranging from 20 to 35 W/m K), showed hot spots temperature variations within 0.5°C, always complying with the requirements.

Measurements

We put a stave prototype, with dummy silicone heaters glued on it, in a cold box, where the ambient temperature was set at -10°C. Then we operated the evaporative cooling system the stave had been connected to, with C3F8 inside as cooling medium. The system was set to have, at the inlet of the stave, the coolant with a quality of 0.3 and a temperature of roughly -22°C. Finally we switched on the heaters and we set the current to dissipate a total power of 143 W. The stave was equipped with thermal sensors, to locally measure the temperature, while the temperature distribution on the surface could be registered by means of an infrared camera (see fig. 16). We found the hot spots on the farthest corners of the modules, respect to the axis of the coolant channel, and the measured maximum temperature difference was 10°C. This result complies with the calculation (see fig. 17), if you consider that they were made with a power load of 100 W, while the measurements were made with 143 W. The infrared picture shows also an unexpected hot area. We noticed such areas on

some of the modules, but in different position; that let us suppose that they could be originated by a bad thermal contact due to a poor conductive glue lay up under the module.

7 CONCLUSIONS

Simulations, tests and measurements on real-scale prototypes showed that an extremely light structure, as it has been designed to minimise the material and then optimise the particle transparency, can withstand the loads, meeting the tight stability requirements. The study covered not only the design, but also the set-up of a complete manufacturing and assembling process. The production of several prototypes proved the feasibility of the design and the repeatability of the results, in view of a small series production of around 200 items, as it is foreseen. The bonding of different composite materials, as carbon-carbon tiles and carbon fibres profiles, showed really satisfactory performances from both strength and stability points of view. The structure under study has been successfully modelled and the model validated by means of cross checks with real scale prototypes measurements. The difference with the calculations are probably due to a treatment (impregnation with resin) of the carbon-carbon part out of standard, that gave its thermal-mechanical properties (CTE) unexpected values. Nevertheless, the model proved to correctly reproduce the physics of the phenomena, then being a good tool to check alternative constraints solutions, different materials and load conditions.

8 REFERENCES

(1) ATLAS Technical Proposal - CERN/LHCC/94-43, CERN, Switzerland, Dec. 15 1994.

(2) ATLAS Pixel Detector Technical Design Report CERN/LHCC/98-13, CERN, Switzerland, May 1998.

(3) Fluorocarbon Evaporative Cooling Developments for the ATLAS Pixel and Semiconductor Tracking Detectors ATLAS-INDET-99-01618, CERN, Switzerland, Sep. 1999.

(4) Precision Measurements and Instruments Corporation: "Thermal expansion measurements of omega and c-c plate specimens", test report of purchase order n° 1334/99, 06/20/00.

(5) Finite Element Analysis, trademarked by: ANSYS Inc., Southpointe, 275 Technology Drive, Canonsburg PA 15301.

(6) M.Olcese, F.Mora, S.Cuneo, A. Vinci, F. Gastaldo, Impregnation process for thin gas-tight carbon-carboncomposite structures, in Proc. 1st PRIME 2001 (International Seminar on PRogress in Innovative Manufacturing Engineering).

(7) “Structural Materials Handbook: Polymer Composites - Vol. 1” – ESA PSS-03-203 Issue 1.

9 LIST OF TABLES

10 LIST OF FIGURES

TAB. 1: design constraints and requirements

ITEM	VALUE	NOTES
Heat to drain	143 W	Evaporative cooling with C3F8
Electronics surface temperature	< -6°C	
Ambient operating temperature	-10°C	Inert atmosphere (N2)
Min/max/fault pressure	2/4/10 bar abs	
Channel hydraulic diameter	4.7 mm	Leak tight channel
Weight to carry	41.5 grams	Uniformly distributed over the length
Assembling accuracy	<±0.25 mm	
Thermal stability	<±0.042 mm	
Moisture stability		To be minimised
Dynamic stability	>100 Hz	First modal frequency
Mass		To be minimised
Life time	10 years	Radiation hard

TAB. 2: material characteristics

MATERIAL	CTE			λ			E			ρ	X_0
	[1/°C]			[W/m °C]			[Gpa]			[Kg/m^3]	[m]
	X	Y	Z	X	Y	Z	X	Y	Z		
C-C	-1e-6	6e-6	-1e-6	200	32	200	185	5	185	1800	0.23
Ciba 420A/B	110e-6	110e-6	110e-6				2.2	2.2	2.2	1120	0.25
C pre-preg	-0.97e-6	5.76e-6	-0.97e-6				320	5.9	5.9	1650	0.25
Aluminium	23e-6	23e-6	23e-6	203	203	203	68.5	68.5	68.5	2700	0.09

TAB. 3: numeric values for finite elements simulation

MATERIAL	**Ex**	**Ey**	**Ez**	**CTEx**	**CTEy**	**CTEz**	**ρ**
	[GPa]	[GPa]	[GPa]	[1/°C]	[1/°C]	[1/°C]	[Kg/m^3]
C pre-preg fibres	358	5.99	5.99	-0.85e-6	0.37e-4	0.37e-4	1650
CIBA 420 A/B	2.2e6	2.2e6	2.2e6	110e-6	110e-6	110e-6	1120
SGL impregnated c-c	100	5	100	-0.966e-6	5.76e-6	-0.966e-	1800
BFG impregnated c-c	185	5	185	-0.966e-6	5.76e-6	-0.966e-	1800
CGL 7018	0.22e-3	0.22e-3	0.22e-3	110e-6	110e-6	110e-6	2500
Silicone	131	131	131	2.3e-6	2.3e-6	2.3e-6	8784

TAB. 4: finite elements modal analysis - modal frequencies

Constraint scheme	Mode	1	2	3	4	5	6	7	8	9
Scheme “A”	f [Hz]	105	237	309	370	572	627	780	853	949
Scheme “B”	f [Hz]	148	313	365	402	629	663	853	904	1002

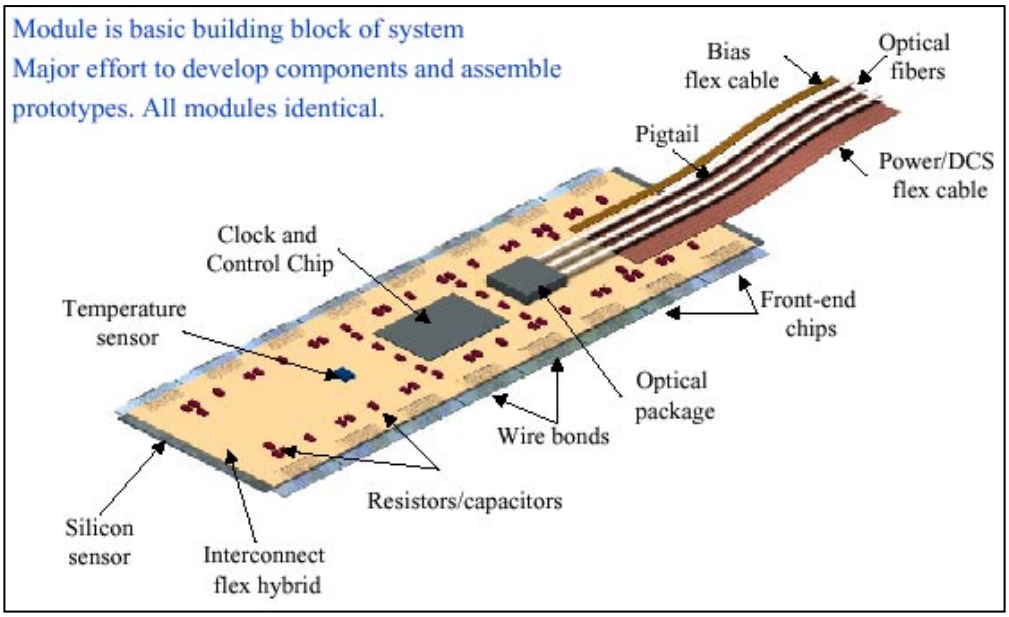

Fig. 1 : Flex hybrid electronic pixel sensor

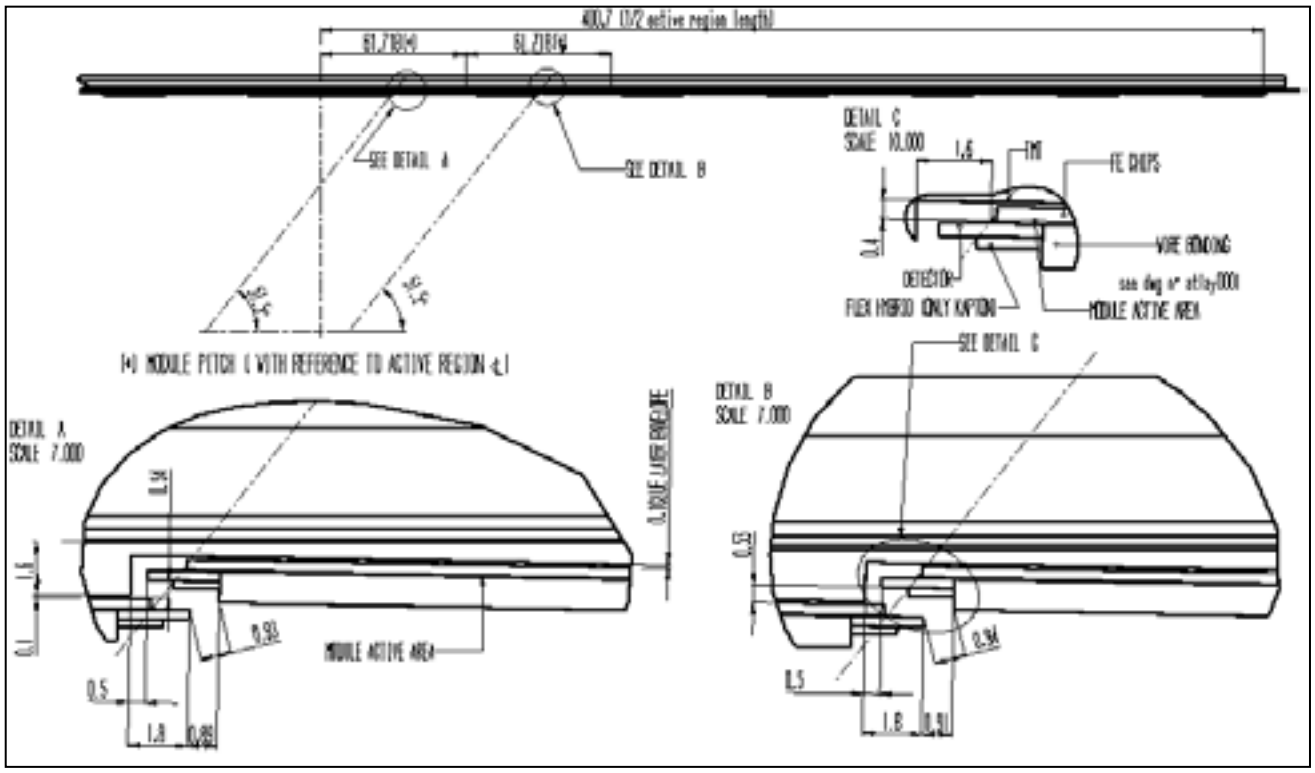

Fig. 2 : Stave modules layout

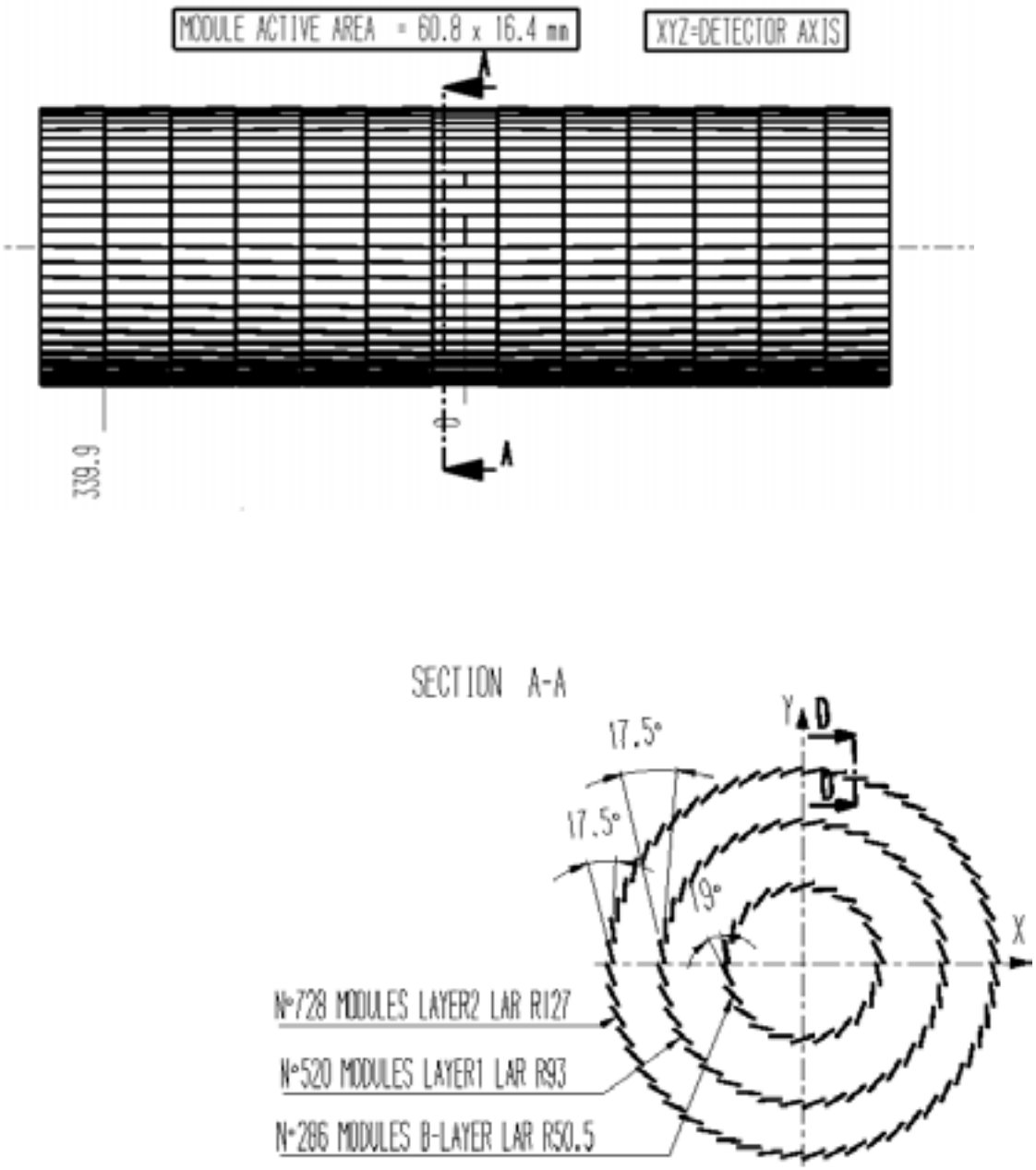

Fig. 3 : Atlas detector barrel active area

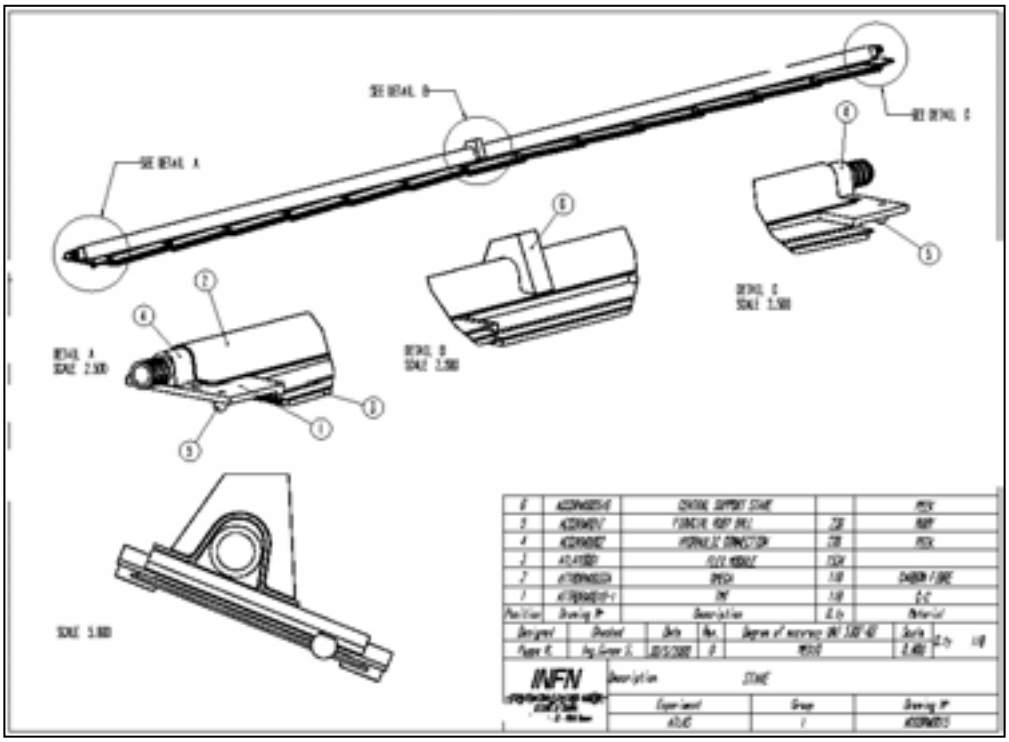

Fig. 4: stave assembly

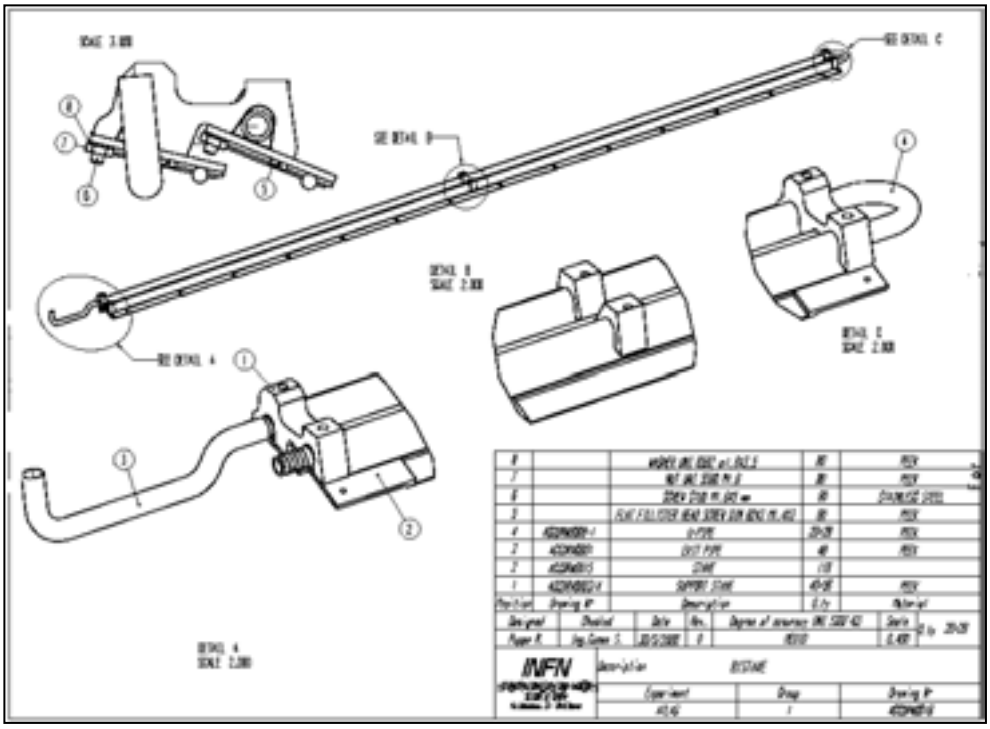

Fig. 5 : Bi-stave assembly

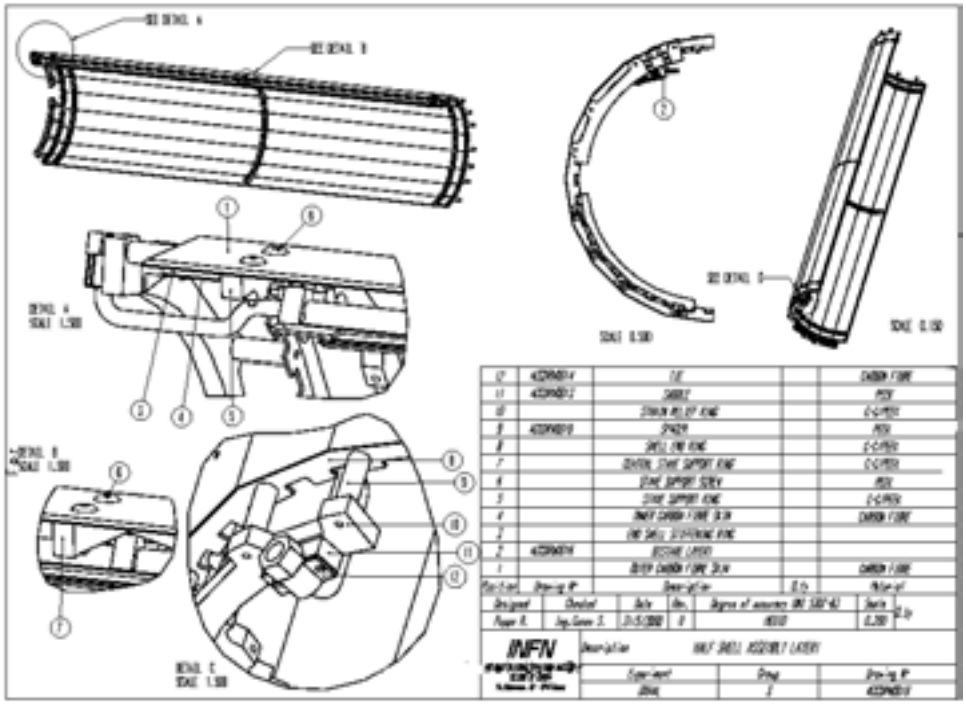

Fig. 6 : Layer assembly

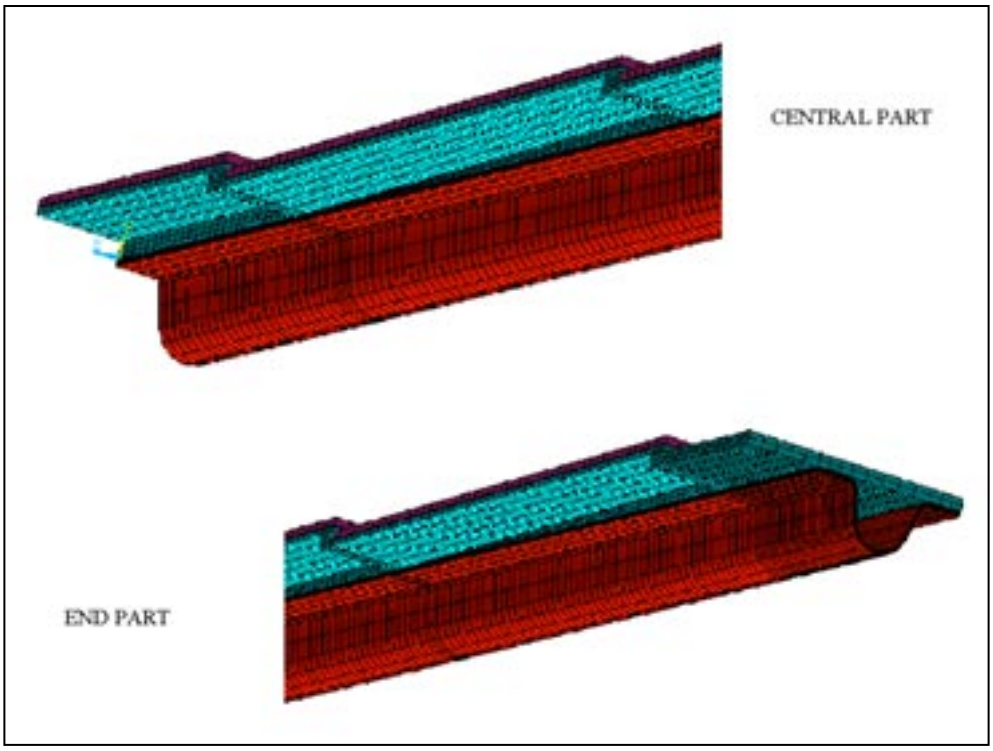

Fig. 7: mesh details.

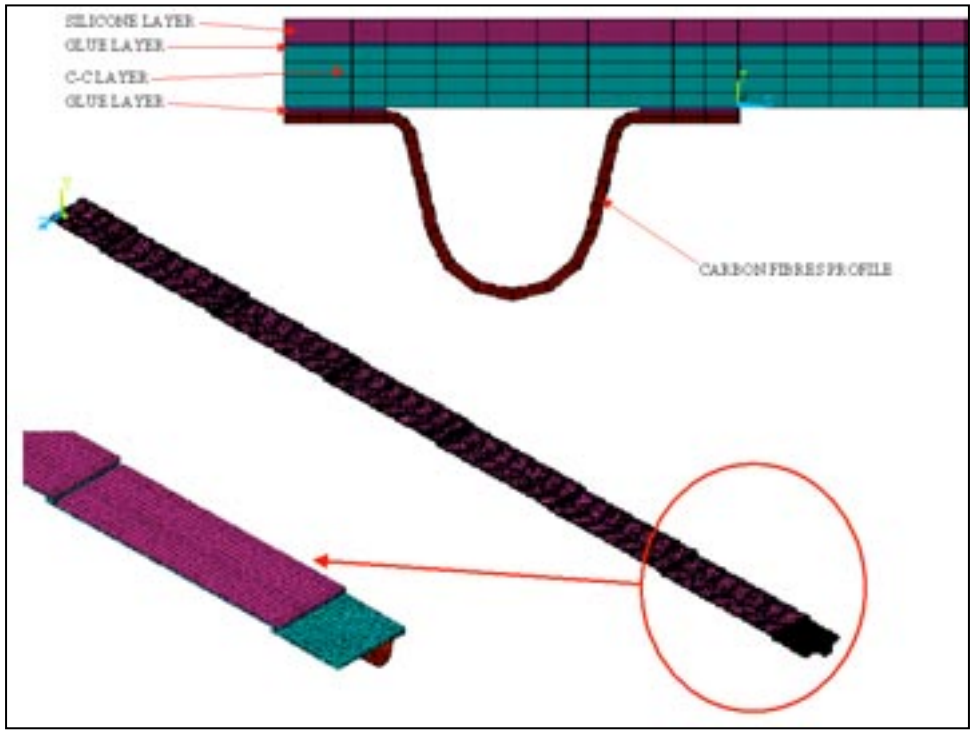

Fig. 8: mesh details – geometry.

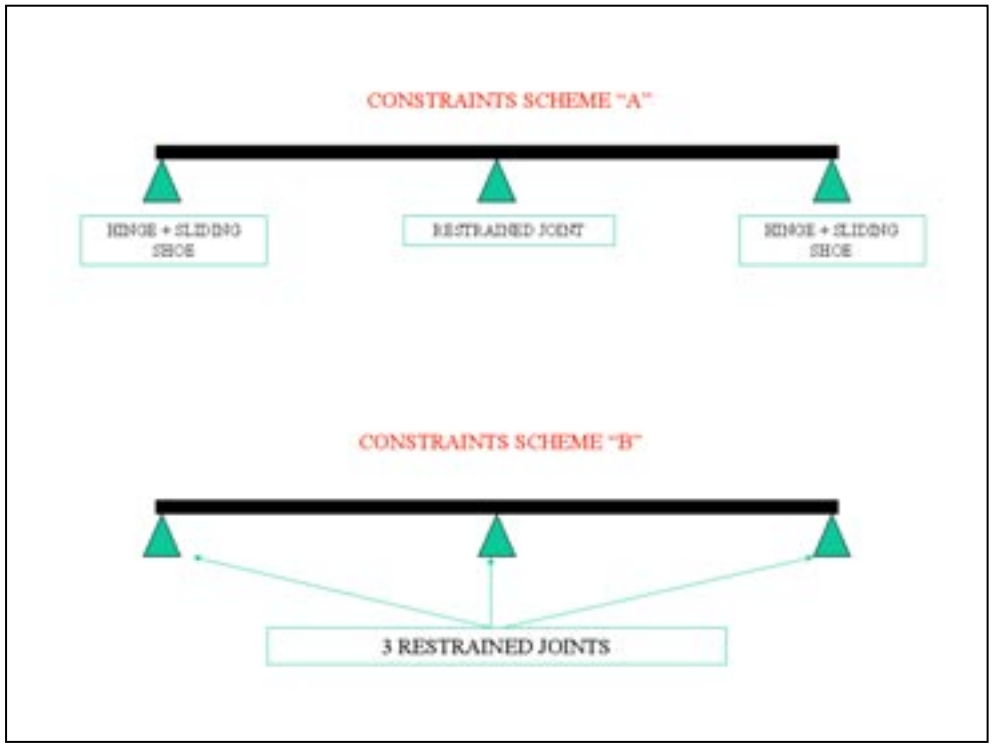

Fig. 9: constraints scheme.

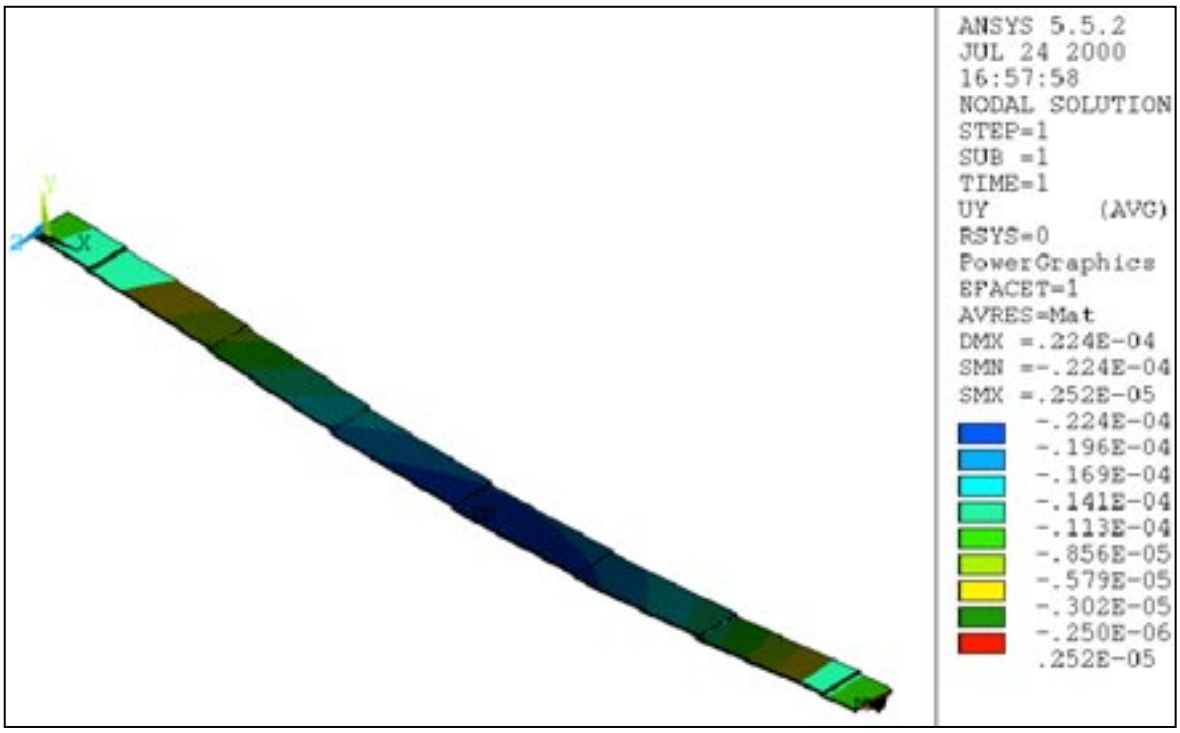

Fig. 10: gravity load simulation (displacements in [m]).

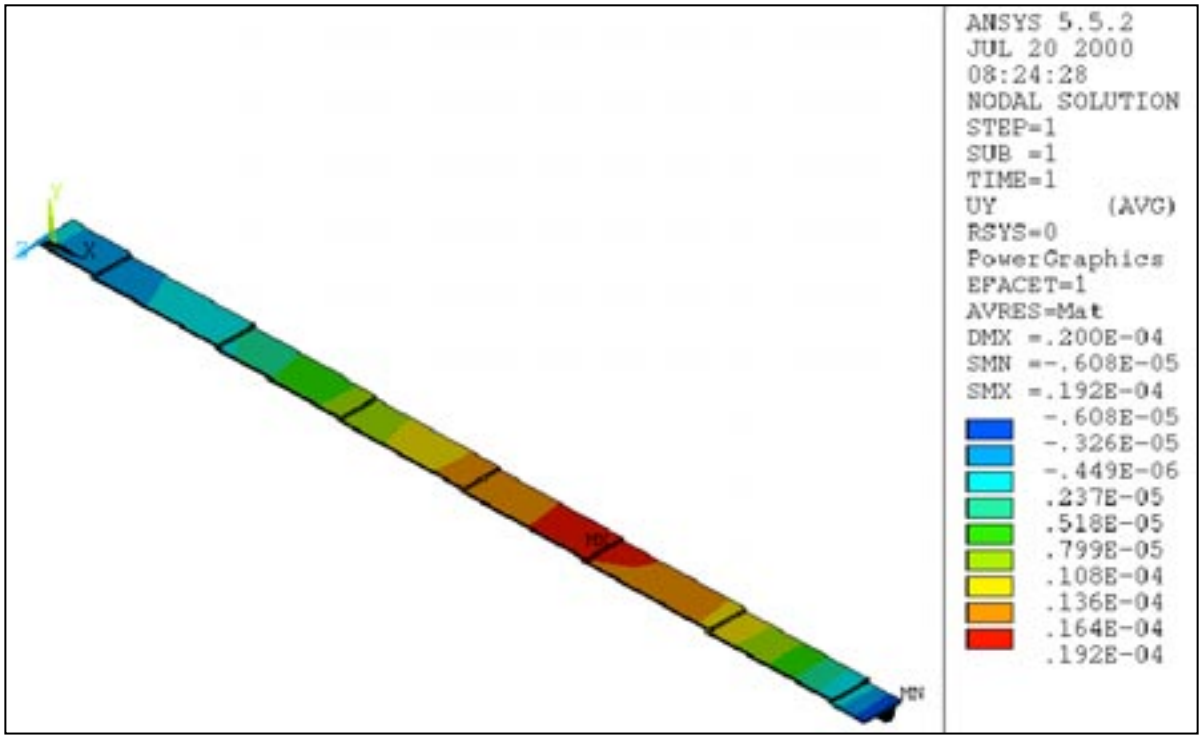

Fig. 11: cool down simulation (displacements in [m]).

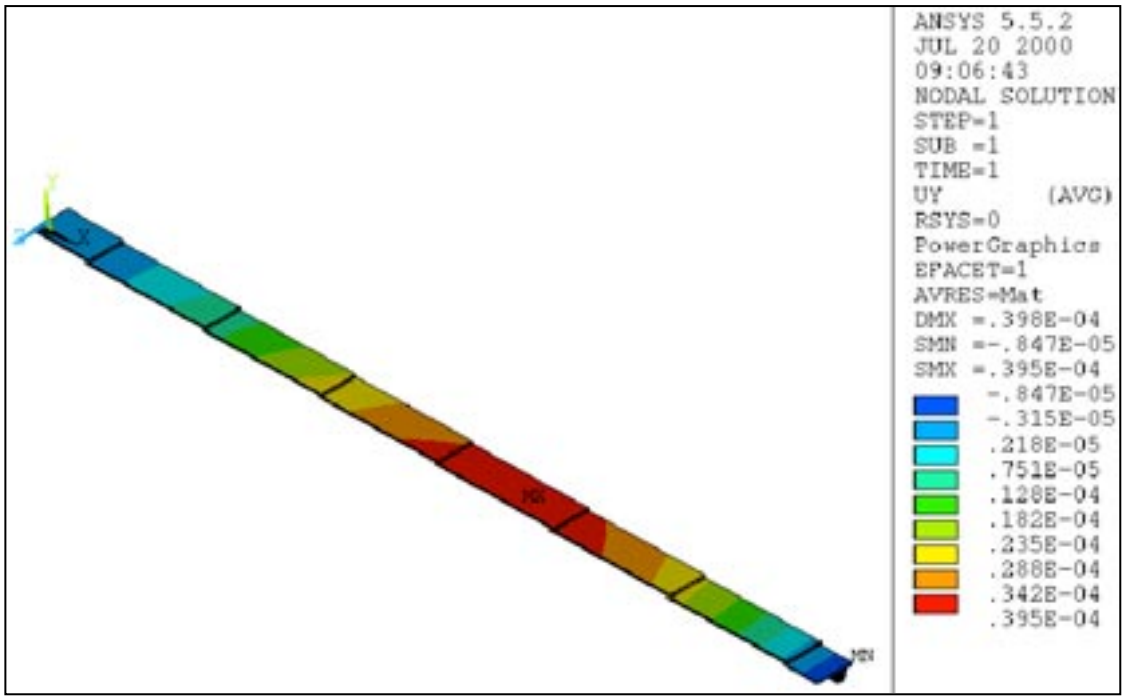

Fig. 12: combined load – gravity against thermal displacements [m].

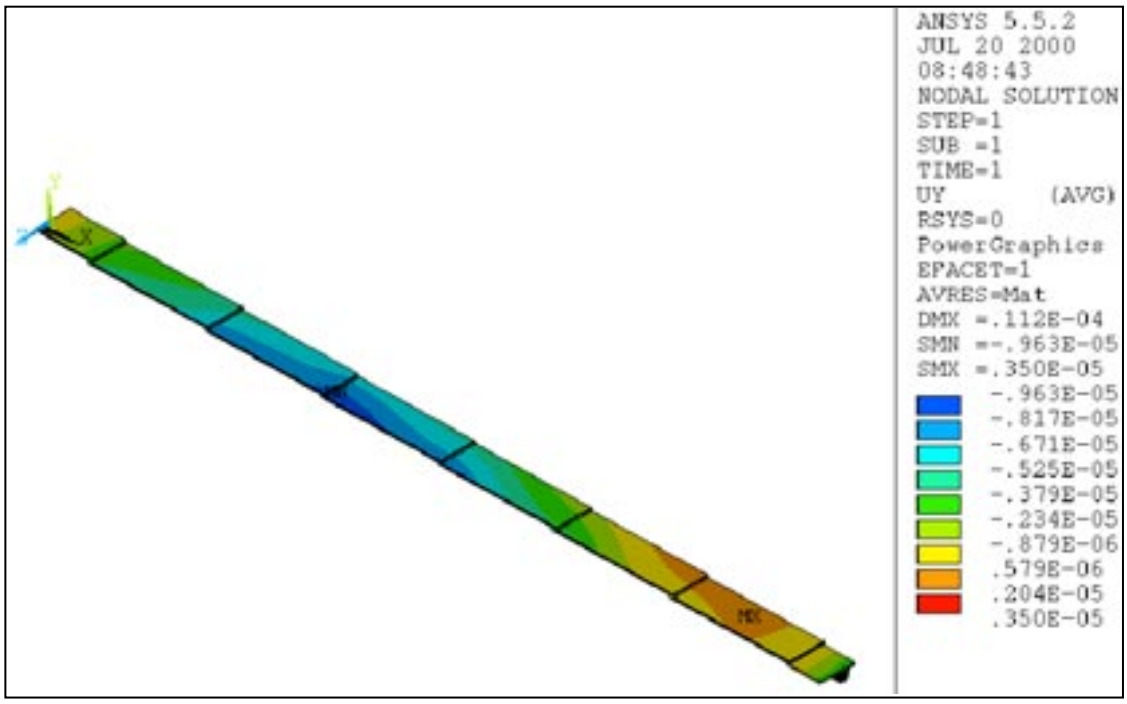

Fig. 13: combined load – gravity against according with thermal displacements [m]).

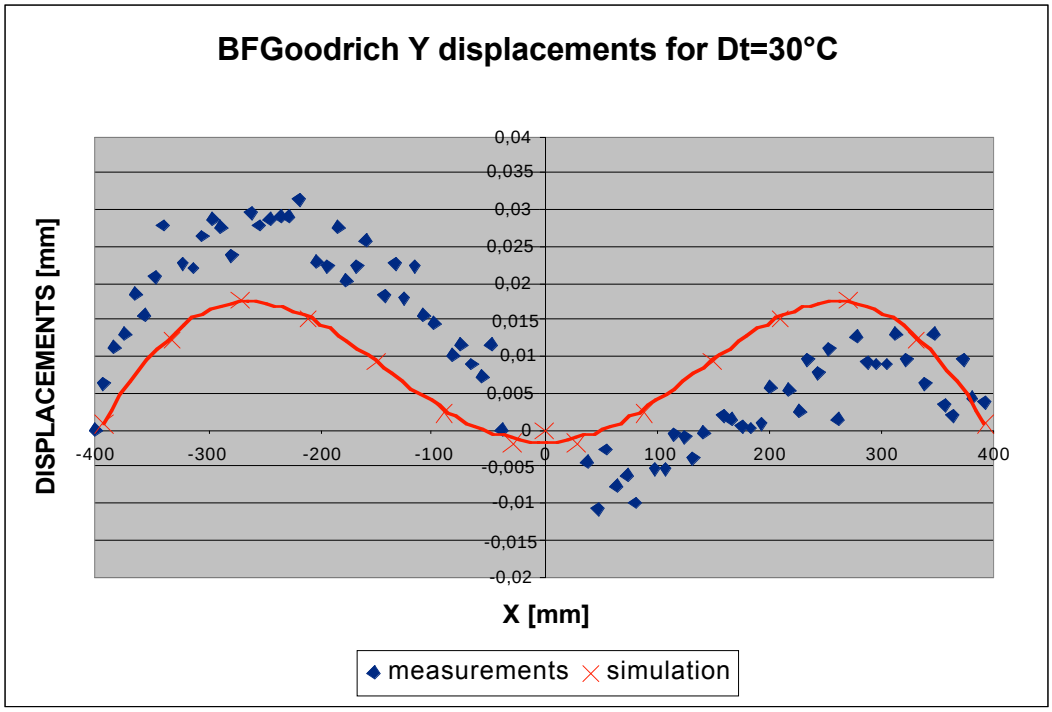

Fig. 14: cool down measurements.

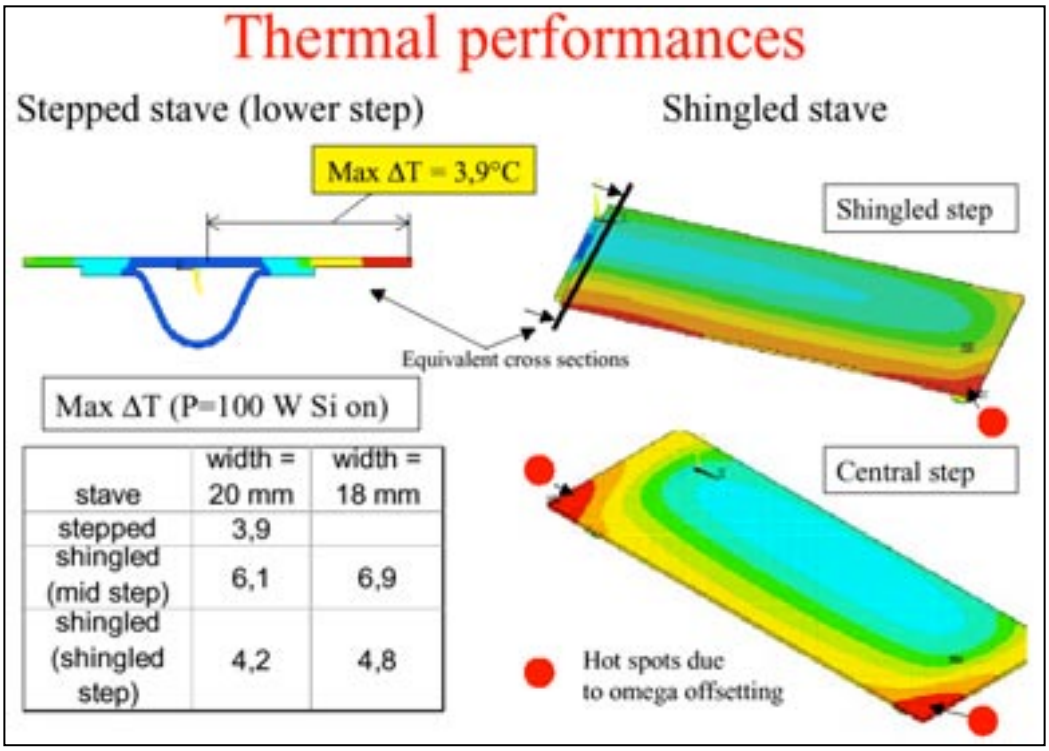

stave	width = 20 mm	width = 18 mm
stepped	3,9	
shingled (mid step)	6,1	6,9
shingled (shingled step)	4,2	4,8

Fig. 15 : calculated temperature distribution on the module surface.

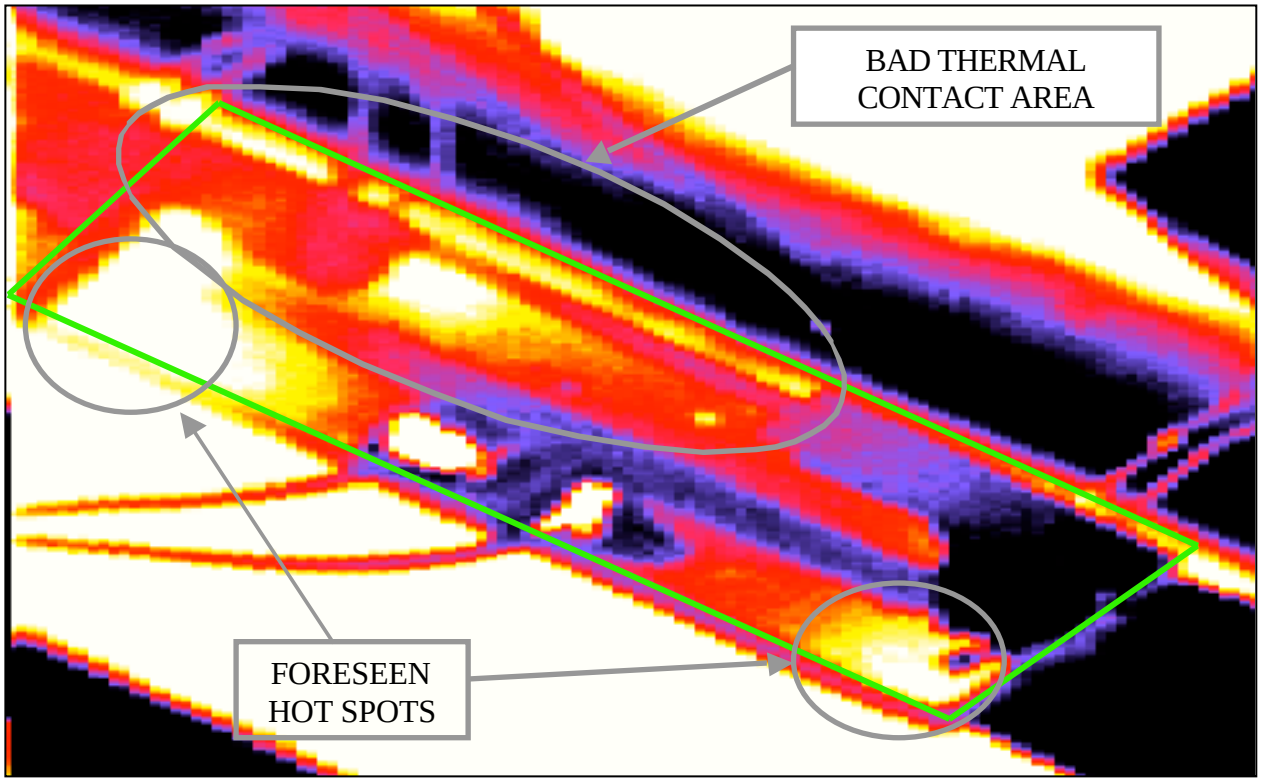

Fig. 16 : measured temperature distribution on a module surface.